Journal of Solid State Chemistry 183 (2010) 1620–1624

Contents lists available at ScienceDirect

Journal of Solid State Chemistry

journal homepage: www.elsevier.com/locate/jssc

Synthesis and structural chemistry of $La_{18}Li_8Rh_4MO_{39}$ (M=Ti, Mn, Ru)

Peter D. Battle [a,*], Siân E. Dutton [a,b], Peter A. van Daesdonk [a]

[a] Inorganic Chemistry Laboratory, Department of Chemistry, Oxford University, South Parks Road, Oxford OX1 3QR, UK
[b] Department of Chemistry, Princeton University, Princeton, NJ 08544, USA

ARTICLE INFO

Article history:
Received 7 April 2010
Received in revised form
5 May 2010
Accepted 6 May 2010
Available online 12 May 2010

Keywords:
Mixed-metal oxides
Neutron diffraction
Cation ordering

ABSTRACT

Polycrystalline samples of $La_{18}Li_8Rh_4MO_{39}$ (M=Ti, Mn, Ru) have been prepared by a solid-state method and studied by neutron powder diffraction. They are isostructural with $La_{18}Li_8Rh_5O_{39}$ and adopt the cubic space group $Pm\bar{3}n$ with a ~12.22 Å. Their structure consists of a La–O framework containing intersecting channels that run along ⟨111⟩. These channels are occupied by chains made up of alternating, face-sharing trigonal-prismatic and octahedral coordination polyhedra; there are two crystallographically distinct types of octahedral site. The prisms are occupied by Li and the transition metals are disordered over the two octahedral sites.

1. Introduction

The crystal structure of $La_{18}Li_8Rh_5O_{39}$[1], shown in Fig. 1, has an intriguing chemical flexibility. In the parent compound, Rh exists as Rh(III) and Rh(IV) in a 4:1 ratio. These cations occupy crystallographically distinct sites, although each has octahedral coordination geometry; the octahedra occupied by Rh(III) are significantly larger than those occupied by Rh(IV). The different octahedral sites alternate along each of the ⟨111⟩ axes of the cubic unit cell, with each pair being separated by a trigonal-prismatic site that is occupied by Li^+. These polyhedral chains fill channels within an infinite network formed by La^{3+} and the remaining oxide ions. The existence of two distinct octahedral sites in the crystal structure prompted us to attempt to prepare new ferrimagnets $Ln_{18}Li_8M'_4MO_{39}$ derived from $La_{18}Li_8Rh_5O_{39}$. In order to induce magnetic ordering we began to synthesize compositions in which both M and M' were magnetic cations from the first transition series, for example $Ln_{18}Li_8Fe_{5-x}Mn_xO_{39}$. We expected the composition x=1 to contain Fe^{3+} and Mn^{4+} cations in a 4:1 ratio and hoped that the superexchange interactions within an ordered array of these d^5 and d^3 cations might give rise to ferrimagnetic behaviour, with a spontaneous magnetisation below some critical temperature. However, a neutron diffraction study of $Nd_{18}Li_8Fe_4MnO_{39}$ [2] showed that the iron and manganese cations are not ordered over the two octahedral sites and below 5 K our ac susceptibility study showed the type of frequency dependence that is associated with spin-glass-like behaviour. To date, it has proved possible to replace Rh completely by Fe [3], or by Fe together with either Mn, Co [2] or Ru [4]; although in some cases the substitution is only successful when there is a concomitant replacement of La by Pr or Nd. Unfortunately, we have observed neither cation nor magnetic ordering in any of these compounds. However, a number of other points of interest have arisen. Attempts to replace Rh by Co alone resulted in the formation of the cation-deficient composition $Nd_{18}Li_8Co_4O_{39}$ [3]. A study of this compound by neutron diffraction found no evidence for the presence of vacancies on the oxygen sublattice, suggesting that the transition metal is present only as Co(IV); the presence of both Fe(III) and Fe(IV) in the iron-containing compositions synthesized to date has been confirmed by Mössbauer spectroscopy [2–4]. The presence of the relatively high oxidation states Co(IV) and Fe(IV), usually formed under high pressure, led to the hypothesis that the framework exerts a chemical pressure on the coordination polyhedra, with the magnitude of the pressure and hence the stability of the compound being determined by the size of the lanthanide (Ln) cation. Further evidence for the compression of the polyhedral chains is provided by the magnetic behaviour of $Nd_{18}Li_8Fe_{5-x}Mn_xO_{39}$ [2] ($0 \le x \le 4$) which is, unusually, consistent with the presence of both low-spin Mn(III) and low-spin Fe(IV). However, the chemical pressure is not high enough to force the Fe(III) cations on the 8e sites into a low-spin configuration.

As part of a wide-ranging investigation of this structural family we have now synthesized $La_{18}Li_8Rh_4MO_{39}$ where M represents Ti, Mn or Ru; elements which frequently occur as M(IV) in mixed-metal oxides. Substitution of 20% of the Rh by an element that can exist as M(IV) is perhaps one of the smallest chemical perturbations that can be imposed on $La_{18}Li_8Rh_5O_{39}$, and these experiments were thus expected to give an indication of the robustness of the cation ordering in this structure. Neutron

* Corresponding author. Fax: +44 1865 272690.
E-mail address: peter.battle@chem.ox.ac.uk (P.D. Battle).

0022-4596/$ - see front matter © 2010 Elsevier Inc. All rights reserved.
doi:10.1016/j.jssc.2010.05.005

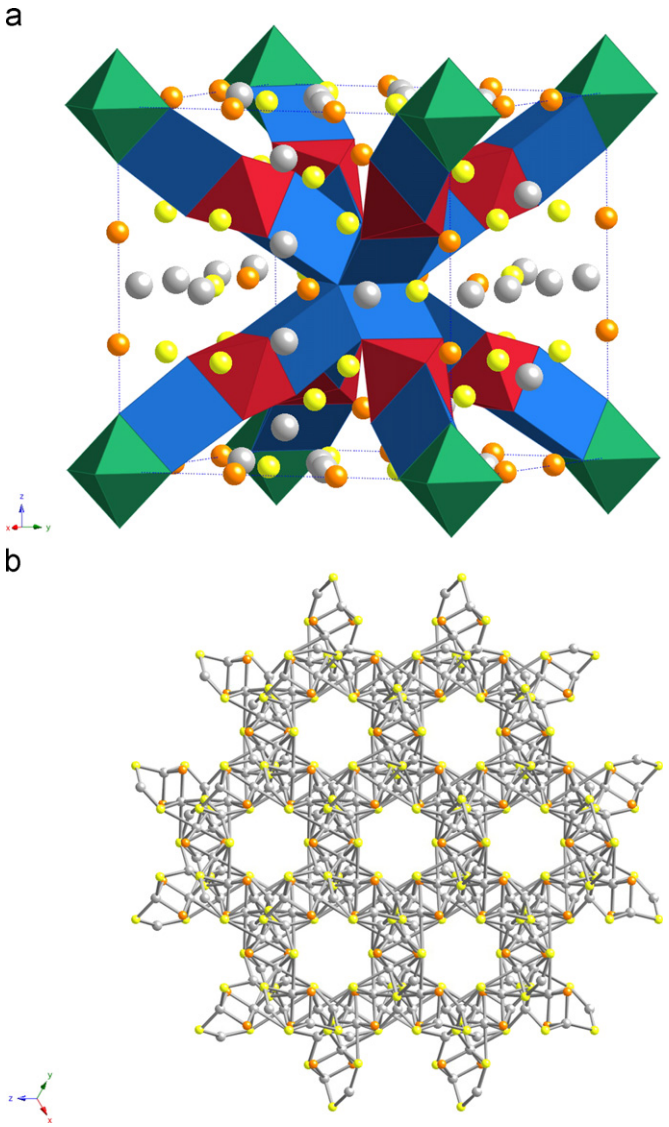

Fig. 1. (a) Polyhedral representation of the cubic (space group $Pm\bar{3}n$) structure of $La_{18}Li_8Rh_5O_{39}$; $LiO(1)_3O(4)_3$ trigonal prisms are blue (16*i* site), $RhO(4)_6$ octahedra are green (2*a*), $RhO(1)_6$ octahedra are red (8*e*), grey circles represent oxygen (O2 and O3), yellow circles La1 and orange circles La2. (b) The La–O2–O3 framework viewed along ⟨111⟩; the polyhedral chains run through the channels. (For interpretation of the references to colour in this figure legend, the reader is referred to the web version of this article.)

diffraction has been used to refine the structures of these three compositions and to determine the distribution of the cations over the available sites. The results of this study are described below.

2. Experimental

Polycrystalline samples of $La_{18}Li_8Rh_4MO_{39}$ (M=Ti, Mn, Ru) were synthesized by grinding together stoichiometric quantities of oxide starting materials (lanthanum(III) oxide (99.99%, Alfa Aesar), rhodium(III) oxide (99.99%, Alfa Aesar), ruthenium(IV) oxide (99.95%, Alfa Aesar), manganese(IV) oxide (99.999%, Alfa Aesar) and titanium(IV) oxide (99.995%, Alfa Aesar)) and a 50% excess of volatile lithium carbonate (AnalaR) prior to firing in pellet form at 800 °C in air for 12 h. A further 50% excess lithium carbonate was ground into the reaction mixture before it was fired again in air for 1 h, as a pellet, at 1000 °C. X-ray powder diffraction was used to monitor the progress of the reactions. Further 1-h firings, with the addition of 50% excess lithium carbonate, were carried out on samples that X-ray powder diffraction showed to be impure at this stage.

All X-ray powder diffraction was carried out on a Philips X′pert diffractometer operating with Cu$K\alpha_1$ radiation with a step size of $\Delta 2\theta = 0.0084^\circ$. High-intensity X-ray powder diffraction data were collected over a small angular range ($15 \le 2\theta/^\circ \le 40$) in an attempt to detect impurities. High-resolution X-ray powder diffraction data for use in quantitative analysis were collected over the angular range $5 \le 2\theta/^\circ \le 125$. The X-ray scattering from these materials is dominated by the heavy metals and consequently it was not possible to perform a full structural analysis using these data. Limited Rietveld [5] refinements were carried out using the GSAS [6] suite of programs in order to determine the unit cell parameters. Backgrounds were fitted using a Chebyshev polynomial of the first kind and the peak shape was modelled using a pseudo-Voigt function.

The diffractometer D2b at the Institut Laue Langevin, Grenoble, France was used to collect neutron powder diffraction data on the M=Ti, Mn compounds using a wavelength of ~1.59 Å. The unit-cell parameters derived from X-ray diffraction data were used to calibrate accurately the neutron wavelength. Data were collected over the angular range $5 \le 2\theta/^\circ \le 160$ with a step size $\Delta 2\theta = 0.05^\circ$ at room temperature. Samples (~0.5 g) were contained within vanadium cans (ϕ=5 mm). Rietveld refinements of the structures were carried out using the FULLPROF [7] program. The background level was refined using the software. Peak shapes were modelled using a pseudo-Voigt function together with a correction for peak asymmetry.

Room temperature neutron diffraction data were collected on $La_{18}Li_8Rh_4RuO_{39}$ using the Polaris time-of-flight (TOF) diffractometer at ISIS, Rutherford Appleton Laboratory, Didcot, UK. Three banks of detectors, positioned at $2\theta = 35^\circ$, 90° and 145°, were used to collect data as a function of TOF, t, over the time period $2 \le t/\text{ms} \le 20$ with a step size of $\Delta t = 0.32$ μs. The sample was contained in a vanadium can. Rietveld refinement of the structure was carried out using the GSAS program; the data collected from each bank of detectors was assigned equal weight in the refinement. The background for all three banks of detectors was modelled using a Chebyschev polynomial function. Peak shapes were modelled using a convoluted Gaussian function with a correction for Lorentzian broadening. A correction for linear absorption by a cylindrical sample was applied to the data from each detector; the absorption was assumed to be inversely proportional to the neutron velocity.

3. Results

3.1. $La_{18}Li_8Rh_4MnO_{39}$

X-ray diffraction showed that our synthesis resulted in a polycrystalline sample of cubic $La_{18}Li_8Rh_4MnO_{39}$, contaminated by a small quantity (~0.007(2) wt%) of Li_2MnO_3.

Our analysis of the neutron diffraction data took as a starting model the structure of $La_{18}Li_8Rh_5O_{39}$, which adopts space group $Pm\bar{3}n$. The smaller octahedral site, labelled in the present case as Rh/Mn1, is located at 0,0,0 and the larger, labelled Rh/Mn2, is located at $\frac{1}{4},\frac{1}{4},\frac{1}{4}$. These are the 2*a* and 8*e* sites, respectively. The smaller site is coordinated by six O4 atoms, which would ideally occupy a 12*f* site but are actually disordered over a 25%-occupied 48*l* *x*,*y*,*z* site, and the larger site is coordinated by six O1 atoms on a crystallographically distinct 48*l* site. The trigonal prismatic site, Li1, is located on *x*,*x*,*x*, a 16*i* site, and is coordinated on one side by

three O4 atoms and on the other by three O1 atoms. Atoms O2 and O3 do not interact strongly with the polyhedral chains; together with the La^{3+} ions they form the channels within which the chains lie. The short La1–O1, La2–O1 and La2–O4 distances within the structure provide links between the chains and the channels. The refinement of the structure of $La_{18}Li_8Rh_4MnO_{39}$ proceeded smoothly using this model, although an additional Li_2CO_3 impurity phase of less than 1 wt% was also detected in the neutron experiment. Refinement of the cation distribution over the two octahedral sites showed Rh and Mn to be disordered over the two positions such that the average scattering factor for the 2*a* position was close to zero. Consequently it was necessary to constrain the isotropic displacement parameter (B_{iso}) at the 2*a* position to an arbitrary value, chosen to be zero. Trial refinements showed that the refined occupation factors were, within reason, insensitive to the value selected. This structural model then gave a good fit to the data, although a relatively large B_{iso} value was observed on the 16*i* trigonal-prismatic site occupied by Li. Refinement of the Li occupancy of the 16*i* trigonal-prism site did not significantly reduce the atomic displacement parameter and hence a stoichiometric composition was assumed. It has previously been reported that in some compositions disorder between Li and the transition metals occupying the 8*e* octahedral site occurs. Structural models in which Rh and/or Mn occupied the prismatic site with the displaced Li occupying the 8*e* octahedral site at $\frac{1}{4}, \frac{1}{4}, \frac{1}{4}$ were therefore considered. The resultant structural models did not significantly improve the fit or reduce the B_{iso} value of the 16*i* trigonal-prismatic site. Hence the site was constrained to be fully occupied by Li with the Rh and Mn cations disordered over the two octahedral sites. The resulting structural parameters and bond lengths are listed in Tables 1 and 2, respectively, and the observed and calculated diffraction profiles are shown in Fig. 2.

Table 1
Structural parameters of $La_{18}Li_8Rh_4MO_{39}$ at room temperature.

		M=Mn	*M*=Ti	*M*=Ru
a (Å)		12.21718(2)	12.22110(8)	12.2382(1)
R_p		0.0345	0.0278	0.0278
La1 24*k*	*y*	0.3050(2)	0.3075(2)	0.30773(8)
0 *y z*	*z*	0.3073(2)	0.3041(2)	0.30401(8)
	B_{iso} (Å^2)	0.84(4)	0.66(3)	0.54(1)
La2 12*f*	*x*	0.3456(2)	0.3470(2)	0.34700(7)
x 0 0	B_{iso} (Å^2)	0.45(5)	0.23(4)	0.29(2)
Rh1(*M*) 2*a*	B_{iso} (Å^2)	0.0	0.0	0.12(4)
0 0 0	Rh occupancy	0.36(1)	0.36(1)	0.41(4)
	M occupancy	0.64(1)	0.64(1)	0.59(4)
Rh2(*M*) 8*e*	B_{iso} (Å^2)	0.37(8)	0.75(8)	0.26(2)
$\frac{1}{4}\frac{1}{4}\frac{1}{4}$	Rh occupancy	0.909(3)	0.909(3)	0.90(1)
	M occupancy	0.091(3)	0.091(3)	0.10(1)
Li1 16*i*	*x*	0.3743(8)	0.3669(6)	0.3721(2)
x x x	B_{iso} (Å^2)	2.8(3)	2.4(3)	1.24(8)
O1 48*l*	*x*	0.8632(3)	0.8636(3)	0.86338(9)
x y z	*y*	0.8598(3)	0.8603(3)	0.85881(9)
	z	0.6937(2)	0.6950(2)	0.69324(6)
	B_{iso} (Å^2)	0.64(3)	0.62(3)	0.59(2)
O2 6*d*	B_{iso} (Å^2)	0.6(1)	1.0(1)	0.78(3)
$\frac{1}{4}\frac{1}{2}$ 0				
O3 12*g*	*x*	0.6310(4)	0.6305(4)	0.6308(1)
x 0 1/2	B_{iso} (Å^2)	0.80(9)	0.57(8)	0.52(2)
O4 48*l*	*x*	0.1529(5)	0.1550(6)	0.1556(1)
x y z	*y*	0.012(2)	0.018(2)	0.0107(5)
	z	−0.011(2)	−0.019(2)	0.0149(4)
	B_{iso} (Å^2)	1.1(2)	2.9(3)	0.94(5)
	Occupancy	0.25	0.25	0.25

Table 2
Bond lengths (Å) in $La_{18}Li_8Rh_4MO_{39}$ at room temperature.

	M=Mn	*M*=Ti	*M*=Ru
La1–O1	2.617(4) × 2	2.642(4) × 2	2.636(2) × 2
	2.697(3) × 2	2.669(3) × 2	2.680(2) × 2
	2.553(4) × 2	2.575(4) × 2	2.5518(7) × 2
La1–O2	2.449(2)	2.495(2)	2.500(1)
La1–O3	2.499(2)	2.485(2)	2.4845(9)
	3.211(2)	3.168(2)	3.1667(2)
La2–O1	2.441(3) × 4	2.440(3) × 4	2.4543(6) × 4
La2–O3	2.474(4) × 2	2.458(4) × 2	2.464(1) × 2
La2–O4	2.363(7)	2.368(7)	2.354(2)
Rh1(*M*)–O4	1.879(7) × 6	1.924(8) × 6	1.917(2) × 6
Rh2(*M*)–O1	2.046(3) × 6	2.049(3) × 6	2.0448(6) × 6
Li1–O1	2.22(1) × 3	2.10(1) × 3	2.198(3) × 3
Li1–O4	2.19(2) × 3[a]	2.22(1) × 3[a]	2.173(4) × 3[a]
Li1–Li1	3.07(1)	3.25(1)	3.130(5)
Rh1(*M*)–Li1	2.66(1)	2.82(1)	2.710(4)
Rh2(*M*)–Li1	2.63(1)	2.47(1)	2.589(4)

[a] Indicates the average distance to the disordered O4 site.

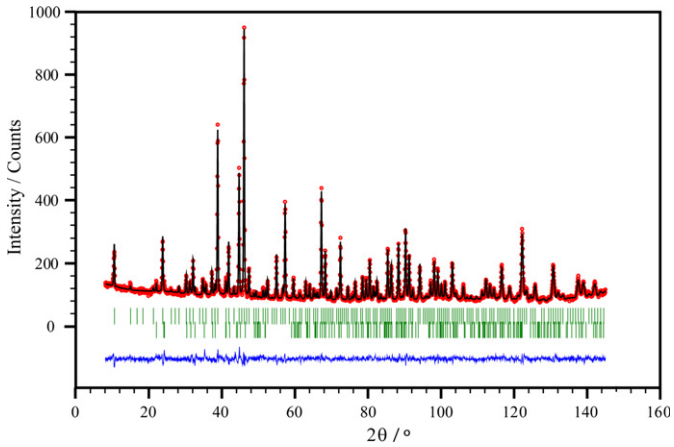

Fig. 2. Observed and calculated neutron diffraction profiles for $La_{18}Li_8Rh_4MnO_{39}$; a difference curve is also shown. The upper and lower sets of vertical bars mark the positions of reflections attributable to $La_{18}Li_8Rh_4MnO_{39}$ and Li_2CO_3, respectively.

3.2. $La_{18}Li_8Rh_4TiO_{39}$

Neutron diffraction data for $La_{18}Li_8Rh_4TiO_{39}$ again revealed a Li_2CO_3 impurity (1.63(6) wt%). The structure of $La_{18}Li_8Rh_4TiO_{39}$ was refined using the same model in the space group $Pm\bar{3}n$. As in the case of $La_{18}Li_8Rh_4MnO_{39}$, the transition metals were found to be disordered over the two octahedral sites with the cation distribution of the 2*a* position such that the neutron scattering length was effectively zero. The atomic displacement factor of this site was therefore fixed to be zero, again with no significant effect on the refined occupancy factors. This structural model gave a good fit to the data, although a large B_{iso} value was observed on the 16*i* trigonal-prismatic site occupied by Li. Structural models in which either Rh and/or Ti displaced Li from the 16*i* trigonal-prismatic site to the 8*e* octahedral position were considered, as was a model in which the overall Li content was allowed to vary. None of these structural models resulted in significant improvements to the fit or a reduction in the atomic displacement parameter of the 16*i* site. The occupancy of the polyhedral network was thus constrained such that Li occupied the trigonal-prismatic 16*i* site with Rh and Ti disordered over the 2*a* and 8*e* octahedral sites. The resulting structural parameters and bond lengths are listed in Tables 1 and 2, respectively, and the observed and calculated diffraction profiles are shown in Fig. 3.

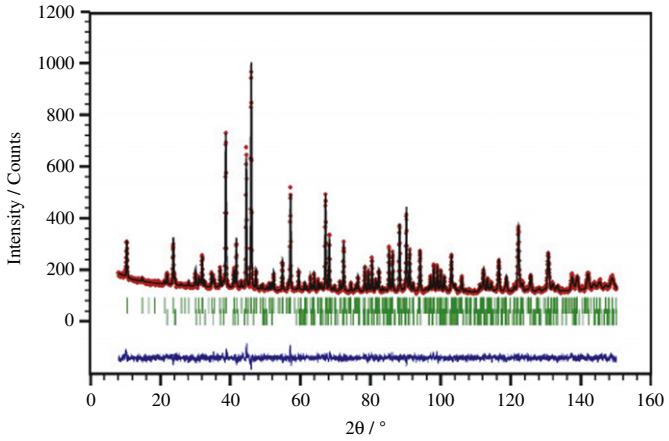

Fig. 3. Observed and calculated neutron diffraction profiles for $La_{18}Li_8Rh_4TiO_{39}$; a difference curve is also shown. The upper and lower sets of vertical bars mark the positions of reflections attributable to $La_{18}Li_8Rh_4TiO_{39}$ and Li_2CO_3, respectively.

3.3. $La_{18}Li_8Rh_4RuO_{39}$

The time-of-flight neutron data showed a small Li_2CO_3 impurity phase (1.1(2) wt%) to be present in the sample. As for the two compositions described above, the structure of $La_{18}Li_8Rh_4RuO_{39}$ was refined using the $La_{18}Li_8Rh_5O_{39}$ structural model in the space group $Pm\bar{3}n$. A model with the Rh and Ru cations disordered over the 2*a* and 8*e* octahedral sites resulted in a good fit to the data with reasonable values for the atomic displacement parameters. More complex structural models were therefore not considered. The structural parameters and bond lengths are listed in Tables 1 and 2, respectively, and the observed and calculated diffraction profiles are shown in Fig. 4.

4. Discussion

The three compounds studied in this work all comprise polyhedral chains contained within a La–O framework. Their structures bear a strong resemblance to that of $La_{18}Li_8Rh_5O_{39}$ which has been described in detail elsewhere [1]. The mean La–O1 distances (2.655, 2.658 and 2.654 Å for M=Mn, Ti and Ru, respectively) show little variation with M, and neither do the La–O2 distances (2.439, 2.435 and 2.442 Å, respectively). They are in good agreement with the distances determined previously [1] in $La_{18}Li_8Rh_5O_{39}$ (2.654 and 2.444 Å). This consistency lends credence to the idea that the lanthanide–oxygen framework is quite rigid, and can act as a host to transition-metal polyhedra of the appropriate size.

As in the case of $La_{18}Li_8Rh_5O_{39}$, but in contrast to many of the isostructural compounds containing iron that have been studied subsequently [2–4], the Li^+ cations in these three compositions are confined to the trigonal-prismatic 16*i* sites and the transition metals are found only on the octahedral sites. This is presumably a consequence of the ratio of the ionic radii of the cations involved. The mean Li–O distances within the prismatic sites are larger than might be expected [8] and the isotropic displacement parameters of the Li^+ cations are also relatively large. These two observations are consistent with the presence of local displacements of the cations off their mean position in the centre of the prism, perhaps in response to the disorder on the O4 site.

Our structure refinements show that cation ordering over the 2*a* and 8*e* sites is incomplete in each of the three compounds studied. However, attempts to introduce higher concentrations of M were always unsuccessful. In the discussion that follows we shall assume that, because of its small size, the 2*a* site is always occupied by tetravalent cations. For the two cases where M is a first-row transition metal, the smaller octahedral site is occupied

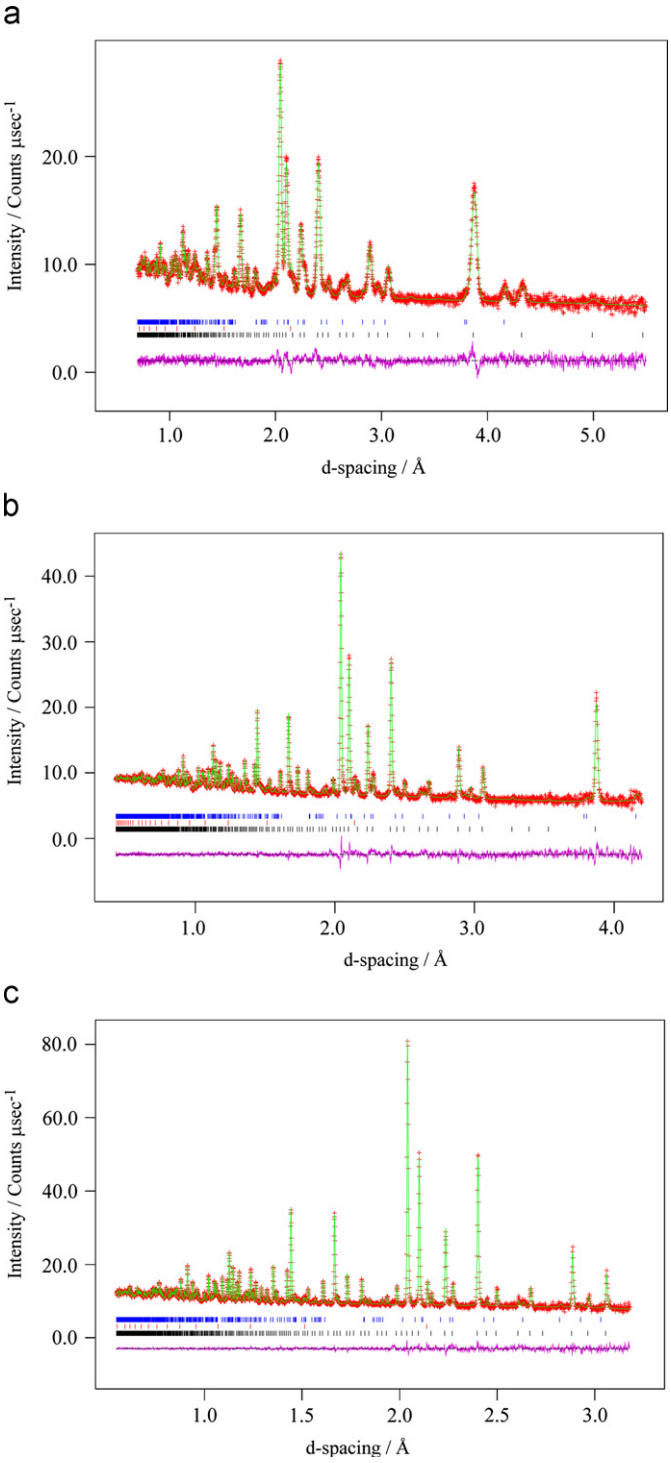

Fig. 4. Observed and calculated neutron diffraction profiles for $La_{18}Li_8Rh_4RuO_{39}$ from the detector banks at (a) 2θ=35°, (b) 2θ=90° and (c) 2θ=135°; the difference curves are also shown. The vertical bars mark the positions of reflections attributable to $La_{18}Li_8Rh_4RuO_{39}$ (black), the V sample can (red) and Li_2CO_3 (blue). The substitution of Ti, Mn or Ru into $La_{18}Li_8Rh_5O_{39}$ results in the loss of the cation ordering seen in the parent compound. (For interpretation of the references to colour in this figure legend, the reader is referred to the web version of this article.)

by Rh and *M* in the ratio 36:64; when *M* is Ru the ratio apparently increases to 41:59, although the relatively low contrast in the neutron scattering lengths of Ru and Rh increases the estimated standard deviation in this case. Before discussing the bond lengths in the newly synthesized compounds it is useful to recall those in some other relevant compounds. More specifically, the Rh–O4 and Rh–O1 bond lengths in the parent compound $La_{18}Li_8Rh_5O_{39}$ are 1.935(3) and 2.048(1) Å, respectively, and the mean *M*–O bond lengths in $SrTiO_3$[9], $SrMnO_3$[10] and $SrRuO_3$[11] are 1.951, 1.889 and 1.984 Å, respectively. These data show that the bond lengths around the 8*e* site are essentially the same in the parent and the new compositions described in this work. In the case of Mn, the reduction in the mean *M*–O4 bond length is consistent with the introduction of the smaller first-row cation, and the bond length found in this study (1.879 Å) is comparable to that in the simple 4H perovskite. However, the lengths of the corresponding bonds when *M*=Ti or Ru (1.924 and 1.917 Å) are shorter than that in $La_{18}Li_8Rh_5O_{39}$, despite the fact that the *M*–O bond lengths in the $SrMO_3$ perovskites are longer than the Rh–O4 bond in the parent compound. We note that the mean Rh/Ru–O4 bond length in $La_{18}Li_8Rh_4RuO_{39}$ is actually shorter than the mean Ru–O distance in many oxides of the Ru(V) cation [12,13]. The contraction of the *M*–O4 bond when Rh is partially replaced by Ru is surprising given their positions in the periodic table; the latter would be expected to be the larger of the two. These data suggest that, particularly in the case where *M*=Ru, an *M*(IV) cation on the 2*a* site will experience a chemical pressure. As described above, the existence of such a pressure in these compositions is consistent with the behaviour of isostructural compounds reported previously. The failure of Ru to occupy exclusively the 2*a* site implies the presence of Ru(III) on 10% of the 8*e* sites. This oxidation state is unusual in oxides synthesized at ambient pressure in air [14–18], although it has previously been invoked to account for the behaviour of the isostructural compound $Pr_{18}Li_8Fe_4RuO_{39}$ [4]; the oxidation states of Fe in that compound were established independently by Mössbauer spectroscopy, leaving little doubt that some of the ruthenium is present in a reduced state. The mean bond lengths around the 2*a* site were 1.90(1) Å, somewhat shorter than in $La_{18}Li_8Rh_4RuO_{39}$. However, the reduction in the mean is understandable given the presence of the smaller, first-row metal.

The disordered distribution of Ti and Rh over the 2*a* site in $La_{18}Li_8Rh_4TiO_{39}$ similarly implies that Ti^{3+} cations occupy ~9% of the 8*e* sites in this compound. Again, this is a cation that is not usually seen in compounds prepared in air, although the concentration is low. It is not possible to glean further information on the cation oxidation states from our neutron diffraction data. X-ray absorption spectroscopy will be used in the future to address these issues in more detail. This technique might also allow us to elucidate the different local environments of the Rh and *M* cations on the 2*a* sites.

We have shown in this study that Ti, Mn and Ru can substitute for 20% of the Rh in $La_{18}Li_8Rh_5O_{39}$. However, we have not seen cation ordering over the 2*a* and 8*e* sites. The parent compound thus remains the only member of this structural family to show complete ordering of two different transition metal cations over the two octahedral sites. (In the case of $Nd_{18}Li_8Fe_5O_{39}$ [3] the 2*a* site was fully occupied by Fe(IV) but neutron diffraction and Mössbauer spectroscopy both showed that Li and Fe(III) were disordered over the 16*i* and 8*e* sites.) Unless this reluctance to order can be overcome, it will be difficult to prepare ferrimagnets based on this structure. Although the absence of ordering is disappointing, we note that these compounds do replicate another interesting feature associated with this structure in that they contain cations in unusual oxidation states, that is Ti^{3+} and Ru^{3+}, albeit in low concentrations.

Acknowledgments

We thank C. Ritter and G. Williams for experimental assistance at ILL and ISIS, respectively, and L. Hutchinson, J. Ray, N. Thammajak and P.A. Williams for assistance in Oxford.

References

[1] P.P.C. Frampton, P.D. Battle, C. Ritter, Inorganic Chemistry 44 (7138) (2005).
[2] S.E. Dutton, P.D. Battle, F. Grandjean, G.J. Long, P.A. van Daesdonk, Inorganic Chemistry 2009 (1613) 48.
[3] S.E. Dutton, P.D. Battle, F. Grandjean, G.J. Long, K. Oh-ishi, Inorganic Chemistry 47 (2008) 11212.
[4] S.E. Dutton, P.D. Battle, F. Grandjean, G.J. Long, M.T. Sougrati, P.A. van Daesdonk, E. Winstone, Journal of Solid State Chemistry 2009 (1638) 182.
[5] H.M. Rietveld, Journal of Applied Crystallography 2 (1969) 65.
[6] A.C. Larson, R.B. von Dreele, General Structure Analysis System (GSAS), LAUR 86-748, Los Alamos National Laboratories, 1994.
[7] J. Rodriguez-Carvajal, Physica B 192 (1993) 55.
[8] P.D. Battle, C.P. Grey, M. Hervieu, C. Martin, C.A. Moore, Y. Paik, Journal of Solid State Chemistry 175 (2003) 20.
[9] Y.A. Abramov, V.G. Tsirelson, V.E. Zavodnil, S.A. Ivanov, I.D. Brown, Acta Crystallographica B 51 (1995) 942.
[10] P.D. Battle, T.C. Gibb, C.W. Jones, Journal of Solid State Chemistry 74 (1988) 60.
[11] C.W. Jones, P.D. Battle, P. Lightfoot, W.T.A. Harrison, Acta Crystallographica C 45 (1989) 365.
[12] P.D. Battle, J.B. Goodenough, R. Price, Journal of Solid State Chemistry 46 (1983) 234.
[13] P.D. Battle, W.J. Macklin, Journal of Solid State Chemistry 52 (1984) 138.
[14] R.J. Bouchard, J.F. Weiher, Journal of Solid State Chemistry 4 (1972) 80.
[15] F.M. da Costa, R. Greatrex, N.N. Greenwood, Journal of Solid State Chemistry 20 (1977) 381.
[16] R. Greatrex, G. Hu, D.C. Munro, Materials Research Bulletin 21 (1986) 797.
[17] N.N. Greenwood, F.D. da Costa, R. Greatrex, Revue de Chimie Minérale 13 (1976) 133.
[18] H. Kobayashi, M. Nagata, R. Kanno, Y. Kawamoto, Materials Research Bulletin 29 (1994) 1271.